

Supporting Information

Table of contents

1. Materials

2. Characterizations and Instrumentation

3. Experimental methods:

- Material synthesis**
- Electrode preparation and electrochemical measurements**

4. Figures and tables

5. References

Materials: Halloysite nanoclay and Nafion® perfluorinated resin solution were procured from Sigma-Aldrich. HCl (37%), HF (48%) and KOH were obtained from Merck. Dopamine hydrochloride was purchased from Alfa Aesar. H₂SO₄ (98 %) was obtained from SD Fine Chemicals. All the chemicals were used as received without any further purification.

Characterizations and Instrumentation: Transmission electron microscopy (TEM) images of the samples were obtained using Technai F30 UHR electron microscope operating at an accelerating voltage of 200 kV. Gas sorption measurements were performed on Autosorb-iQ₂ (Quantachrome corp.) at 77 K and prior to analyses the synthesized samples were degassed under high vacuum for 12 h at 423 K. Ultrahigh pure N₂ (99.9995%) were used in all the measurements. Field emission scanning electron microscopy (FESEM) images of the samples were acquired on Nova-Nano SEM-600 (FEI, Netherlands). X-ray photoelectron spectroscopy analyses were performed using Omicron photoelectron spectrometer equipped with Al K α ($h\nu = 1486.6$ eV) as the X-ray source. Jobin Yvon LabRam HR spectrometer having 632 nm Ar laser was used for acquiring Raman spectra of the samples. Electrochemical measurements were carried out using electrochemical work station obtained from CH instruments (660C, USA) for evaluating the electrochemical activities of the synthesized materials towards hydrogen evolution reaction (HER) and oxygen reduction reaction (ORR). Inductively coupled plasma optical emission spectroscopy (ICP-OES) analyses were performed on Perkin-Elmer Optima 7000DV instrument.

Experimental Methods:

Synthesis of NDC: 235 mg of halloysite clay was dispersed in 250 mL of 10 mM TRIS buffer (pH 8.5) and was sonicated for 30 min. Thereafter, 155 mg of dopamine hydrochloride was added to

above dispersion and was sonicated for 5 min and then left to stir for 22 h at room temperature. Polydopamine coated halloysite clay was obtained after centrifugation and repeated wash with water and ethanol. Further pyrolysis at elevated temperature under Ar for 4 h and subsequent sequential demineralization with 15 mL HCl (6 M) and 15 mL HF (12 M) for 12 h each and thorough washing with water-ethanol resulted in different NDCs (viz. NDC-700, NDC-800 and NDC-900; where the numbers denote the temperatures of pyrolysis in $^{\circ}\text{C}$). The final yield of NDCs was about 30 mg (20 wt.% in terms of carbon precursor, dopamine hydrochloride).

Electrode preparation and electrochemical measurements: The electroactive material (2 mg) was ultrasonically dispersed in water (0.70 mL) and isopropanol (0.30 mL) mixture containing 10 μL of 5 wt. % Nafion[®] solution until a homogeneous catalyst ink was obtained. Thereafter, 10 μL of above dispersion was drop-casted onto a pre-cleaned glassy carbon electrode (GCE) with 3 mm diameter resulting in a catalyst loading of \sim 0.28 mg cm^{-2} . The catalyst modified GCE was dried under ambient conditions which served as a working electrode (WE).

Electrochemical measurements were carried out using a standard three-electrode cell using large area Pt foil as a counter electrode and saturated calomel electrode (SCE) as a reference electrode for studying HER activity in acidic medium (1 M H_2SO_4) and mercury-mercuric oxide electrode was used for evaluating ORR activity in basic medium (0.1 M KOH). For HER, separate measurements were performed in H-type cell wherein working and reference electrodes were kept in one compartment while Pt counter electrode was kept in the other in order to avoid any artifact arising from dissolution of Pt and deposition of the same on the working electrode. All

the polarization curves were corrected for iR losses arising due to ohmic resistance of the cell and the measured potentials vs. SCE or Hg/HgO were calibrated with respect to reversible hydrogen electrode (RHE). The obtained current densities were normalized to geometrical area of the GCE. Linear sweep voltammograms were recorded in 1 M H₂SO₄/ 0.1 M KOH at a scan rate of 5 mV s⁻¹ in O₂/N₂ saturated aqueous electrolytes. Cyclic voltammograms (CV) were recorded under similar conditions and at different scan rates (20-200 mV s⁻¹) between -0.10 V and 0.40 V (vs. RHE) in order to evaluate electrochemical double layer capacitance (C_{dl}), representing electrochemically active surface area (ESCA).

Calculation of electron transfer number from Koutecky-Levich equation for oxygen reduction reaction (ORR): Rotating disk electrode data was used to determine number of electrons transferred per O₂ molecule using Koutecky-Levich equation:

$$\frac{1}{j} = \frac{1}{j_k} + \frac{1}{j_l} = \frac{1}{j_k} + \frac{1}{B\omega^{1/2}} \quad (1)$$

Where j is the measured current density, j_k and j_l are the kinetic and diffusion limited current densities respectively and ω is the electrode rotation speed. B is Levich slope and is determined from Koutecky-Levich plots using below equation (2):

$$B = 0.62nFC_{O_2}(D_{O_2})^{\frac{2}{3}}\nu^{-\frac{1}{6}} \quad (2)$$

Where n is the number of electron transferred per O₂ molecule, F is the Faraday constant (96485 Cmol⁻¹), C_{O_2} is the bulk concentration of O₂ in the electrolyte, D_{O_2} is the diffusion coefficient of O₂ and ν is the kinematic viscosity of the electrolyte.

Calibration of reference electrodes:

The reference electrodes (SCE and Hg/HgO), used in different media were calibrated with respect to reversible hydrogen electrode using large area Pt foil as a working and counter electrodes. High purity hydrogen gas was purged in the respective solutions for atleast 45 min before the experiments and thereafter a constant overhead purge was maintained during the measurements.

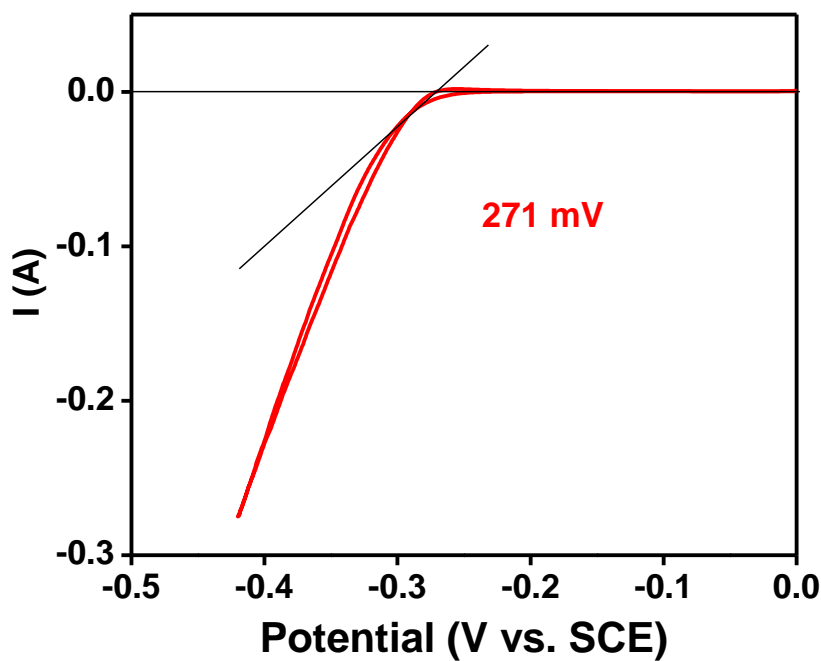


Figure S1. Calibration of saturated calomel electrode (SCE) with respect to reversible hydrogen electrode (RHE) in 1.0 M H₂SO₄ at 1 mV s⁻¹.

Therefore, we have for 1.0 M H₂SO₄:

$$E_{\text{RHE}} = E_{\text{SCE}} + 0.271 \text{ V}$$

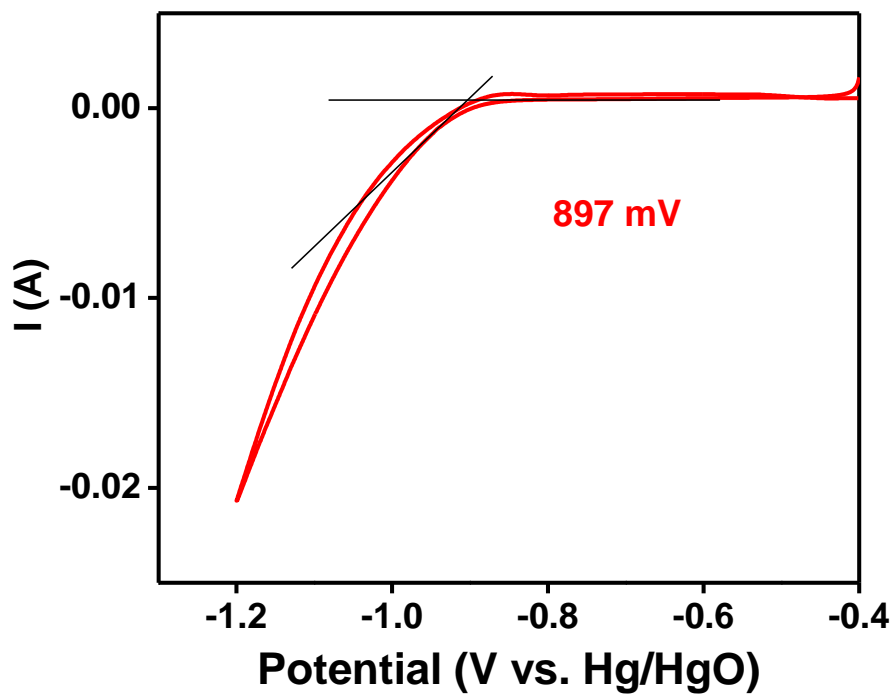


Figure S2. Calibration of mercury/mercury oxide (Hg/HgO) electrode with respect to reversible hydrogen electrode (RHE) in 0.1 M KOH at 1 mV s⁻¹.

Therefore, we have for 0.1 M KOH:

$$E_{\text{RHE}} = E_{\text{Hg/HgO}} + 0.897 \text{ V}$$

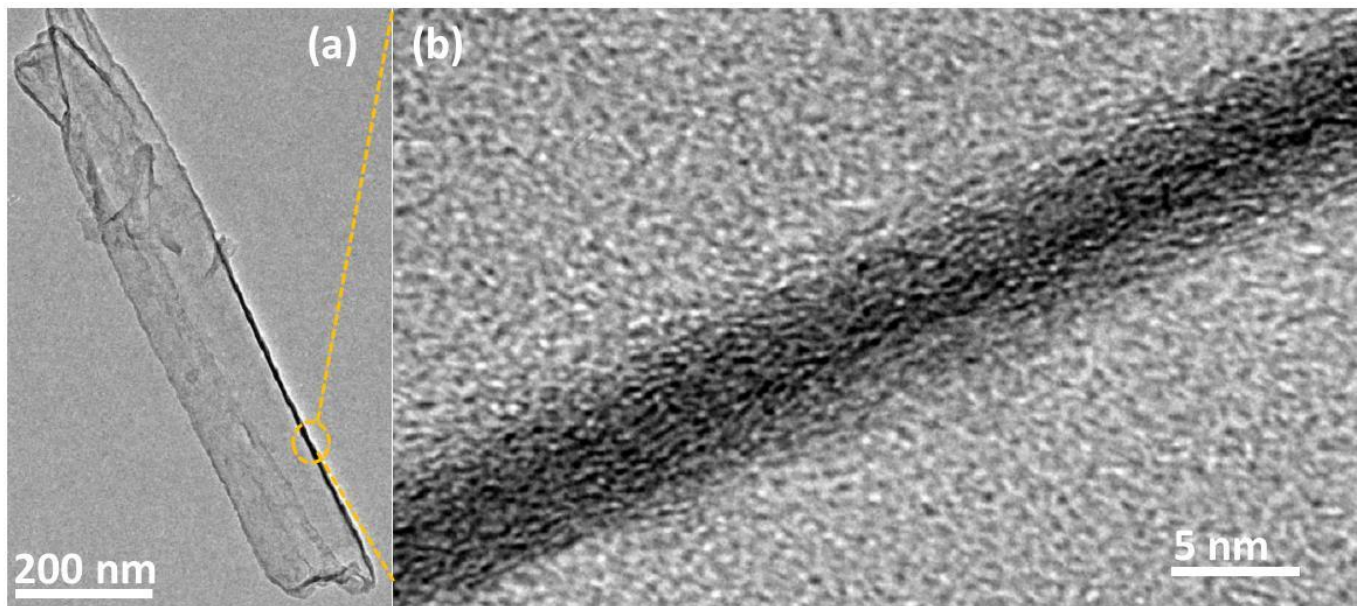


Figure S3. (a) TEM images of NDC-800 and (b) shows HRTEM image of the region circled in dotted lines in (a) indicating graphitic nature of the carbon walls.

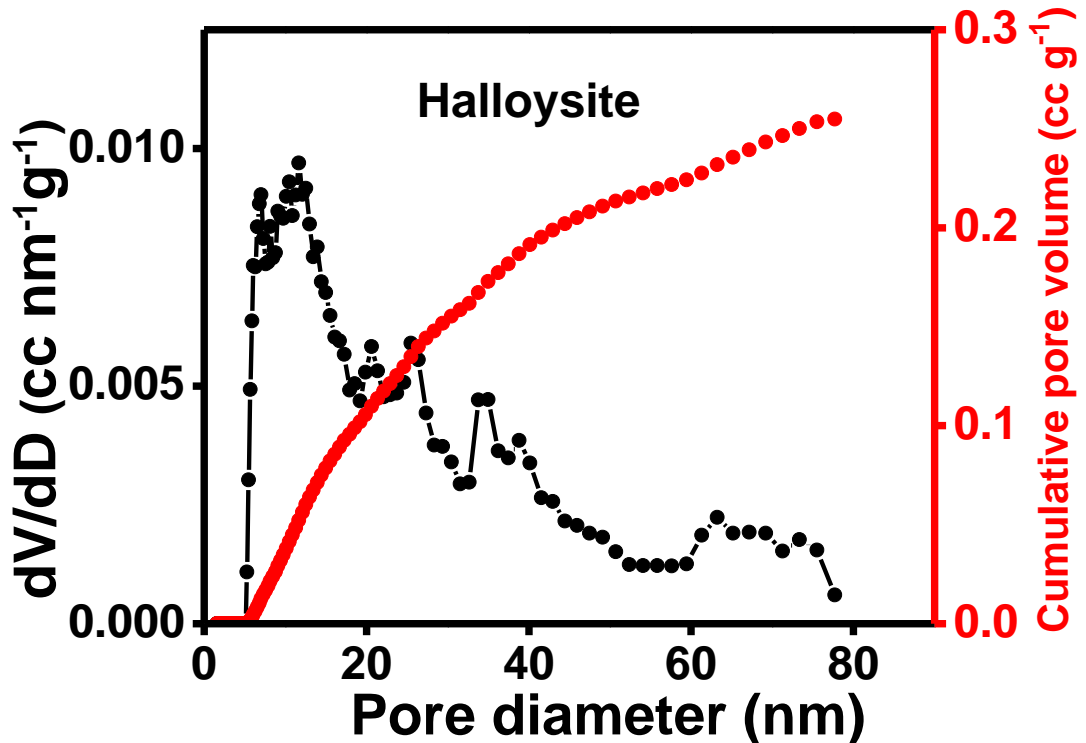


Figure S4. Pore size distribution of halloysite clay along with cumulative uptake obtained via NLDFT (Non-local density function theory) method.

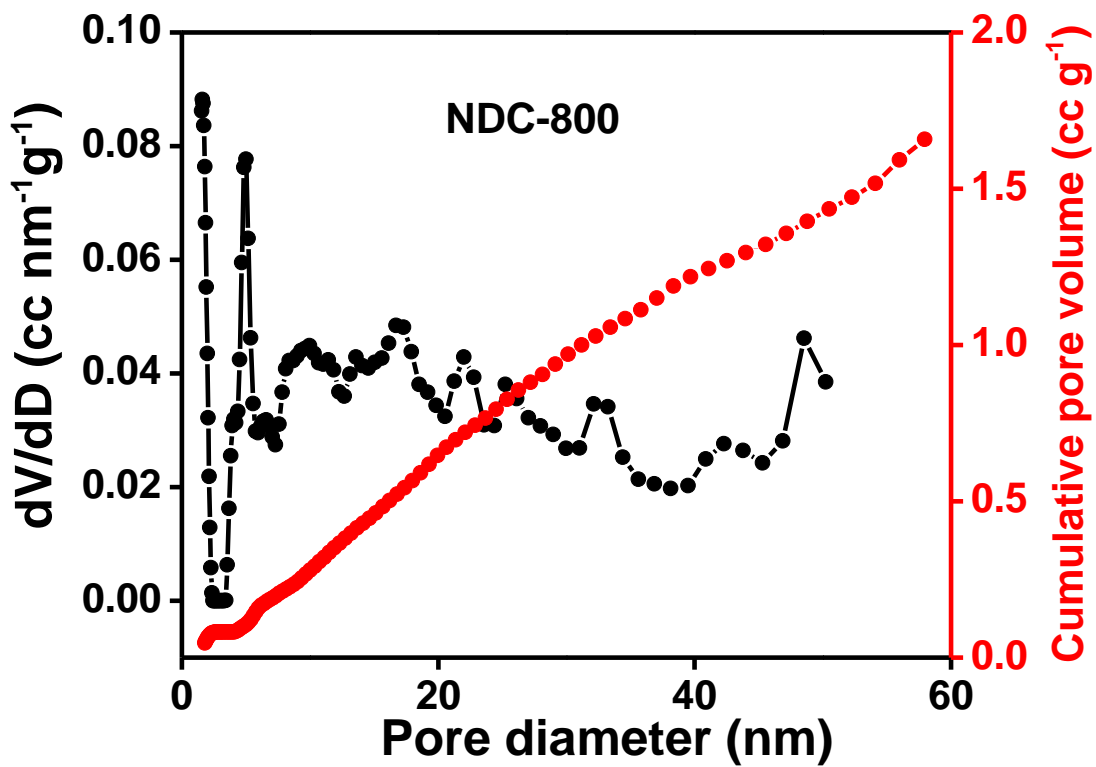


Figure S5. Pore size distribution of NDC-800 along with corresponding cumulative pore uptake calculated by QSDFT (Quenched solid density function theory) method.

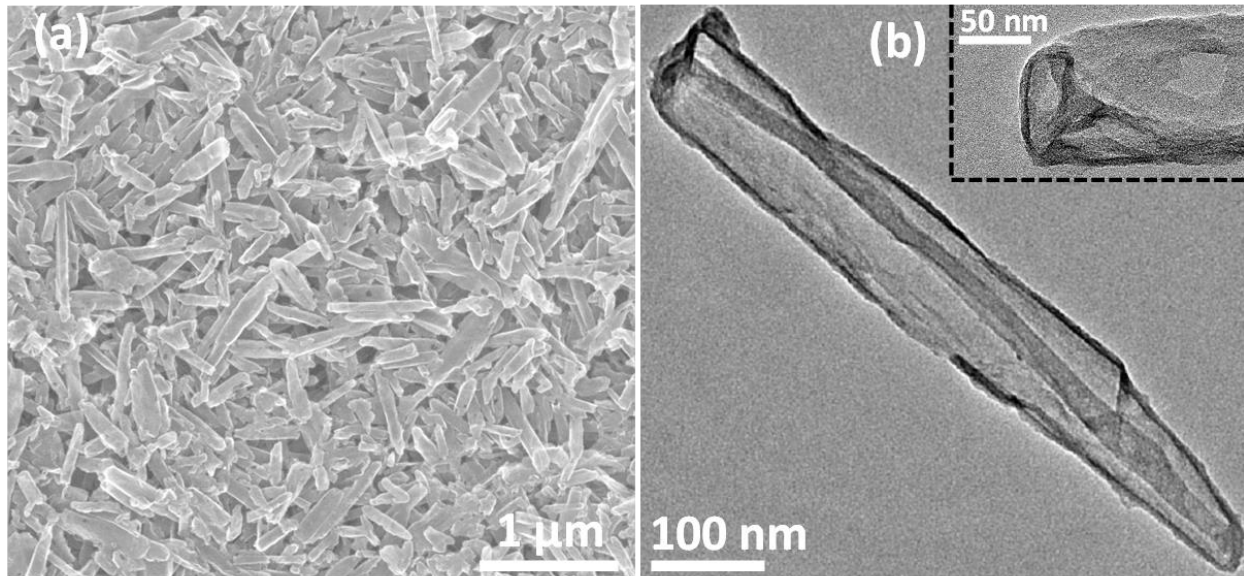


Figure S6. (a) FESEM images of NDC-700 indicating faithful morphological replication of parent halloysite clay and (b) TEM image of NDC-700 indicating tubular structure (inset shows tubular opening).

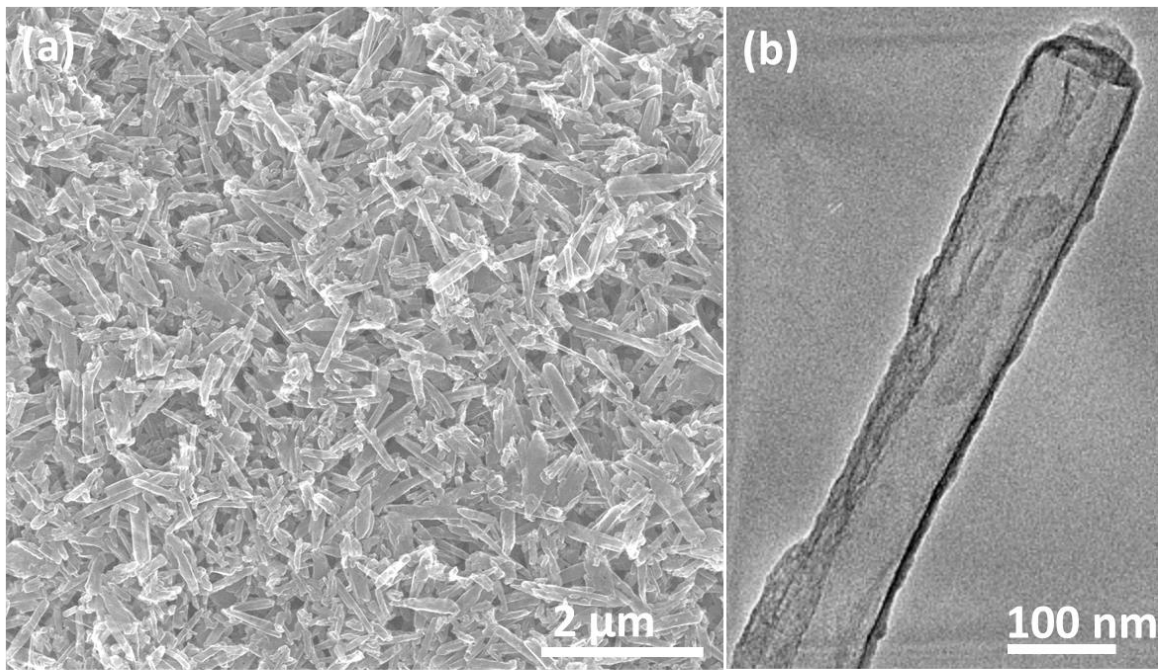


Figure S7. (a) FESEM and (b) TEM images of NDC-900 indicating tubular morphology.

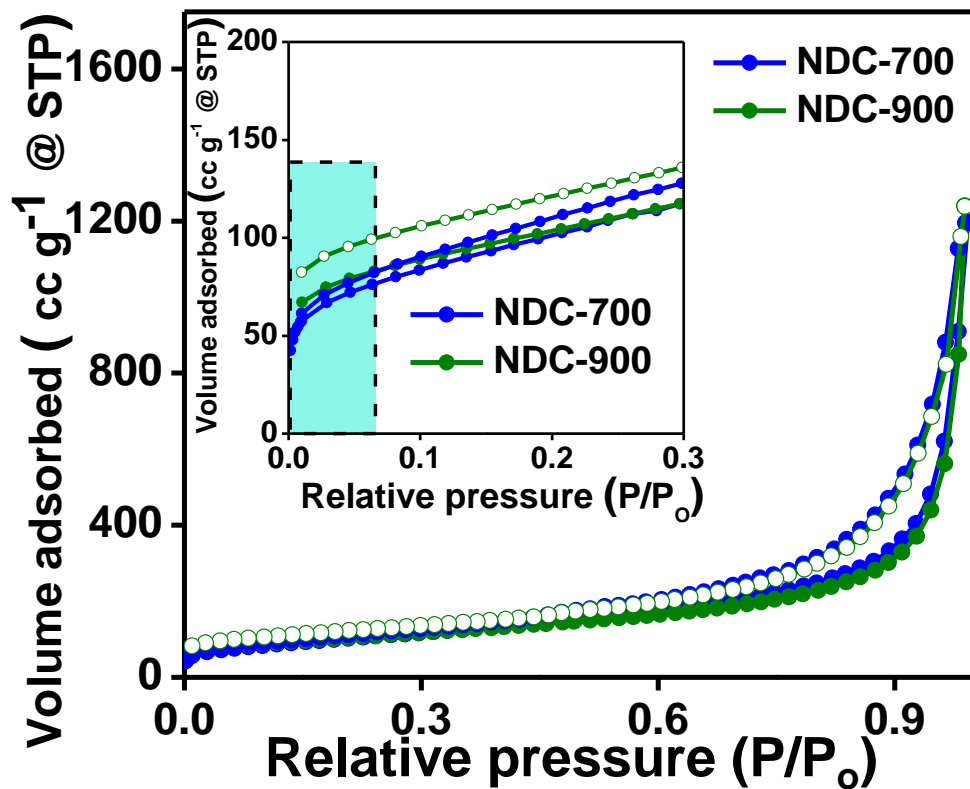


Figure S8. N_2 adsorption-desorption isotherms of NDC-700 and NDC-900; inset indicate microporous nature of the NDCs.

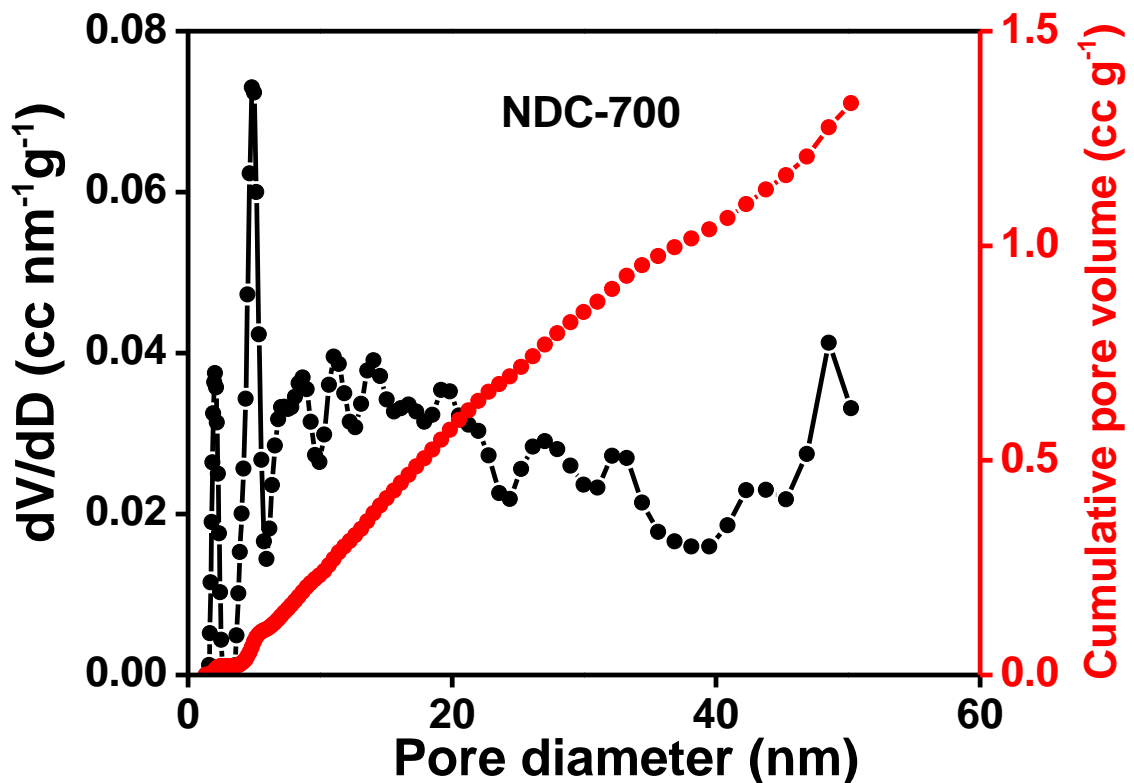


Figure S9. Pore size distribution of NDC-700 along with corresponding cumulative pore uptake calculated by QSDFT method.

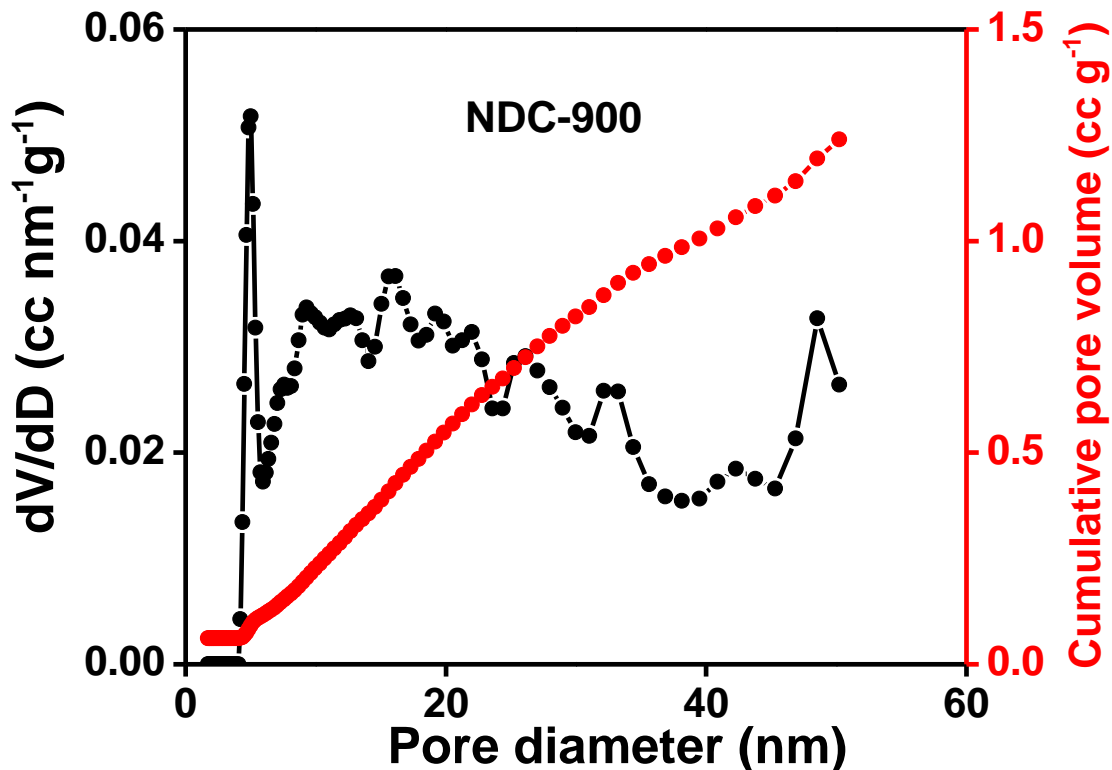


Figure S10. Pore size distribution of NDC-900 along with corresponding cumulative uptake obtained via QSDFT method.

| Materials | S_{BET}^a ($m^2 g^{-1}$) | V_T^b ($cm^3 g^{-1}$) | D_{meso}^c (nm) |
|-------------------|---------------------------------|------------------------------|----------------------|
| Halloysite | 52 | 0.228 | >15 |
| NDC-700 | 373 | 1.406 | >15 |
| NDC-800 | 570 | 1.879 | >15 |
| NDC-900 | 368 | 1.313 | >15 |

Table S1. Textural parameters of halloysite nanoclay and NDCs.

^a BET (Brunauer-Emmett-Teller) specific surface area calculated in the relative pressure (P/P_0) range of 0.5 to 0.27, ^b Total pore volume was calculated at $P/P_0 = 0.97$ and ^c mesopore diameter calculated by QSDFT/NLDFT method.

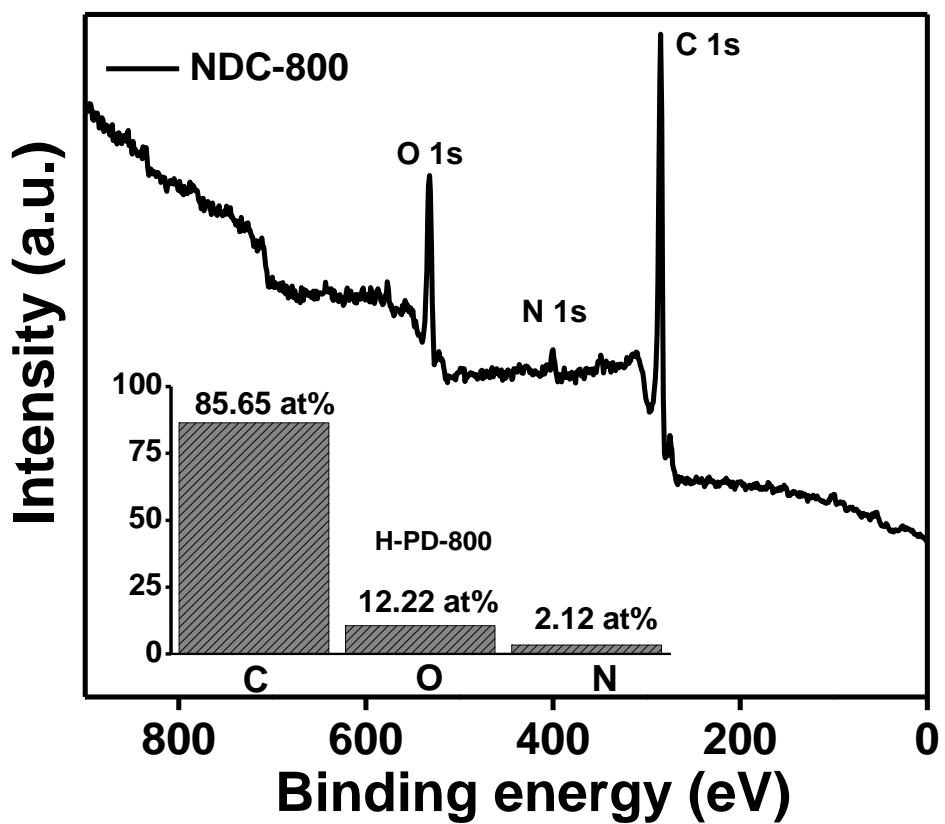


Figure S11. XPS survey spectrum of NDC-800; inset shows corresponding elemental content in atomic percentages.

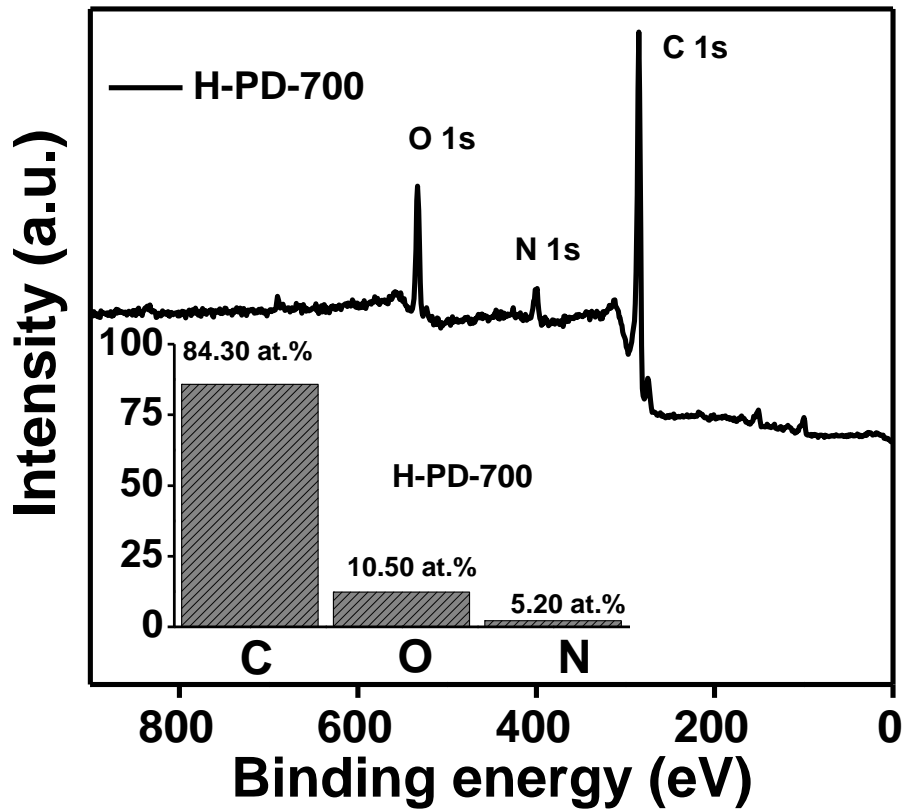


Figure S12. XPS survey spectrum of NDC-700; inset shows corresponding elemental content in atomic percentages.

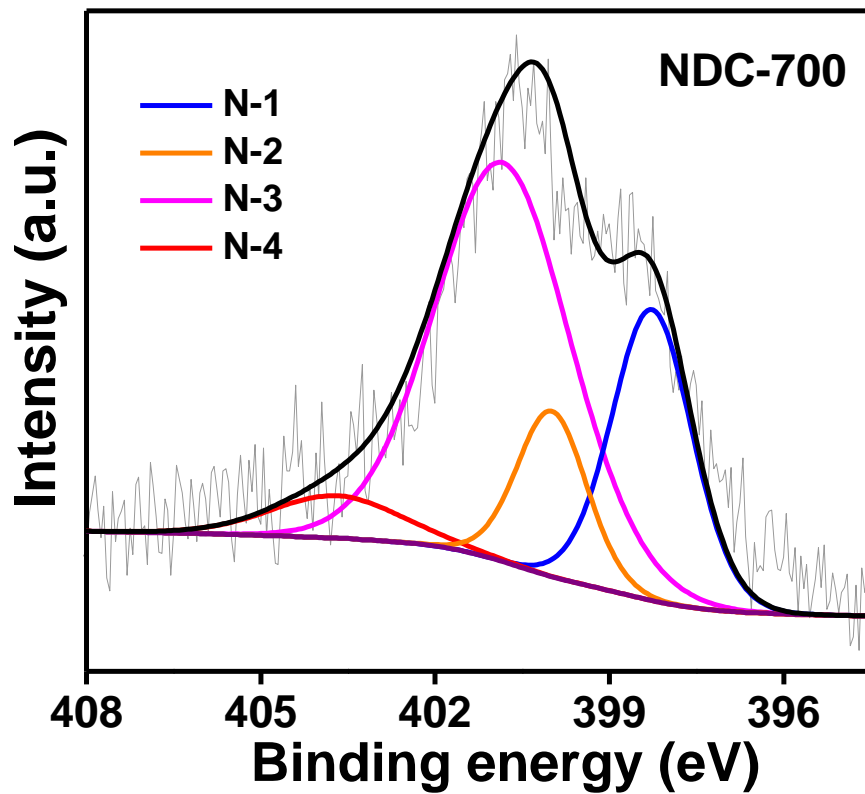
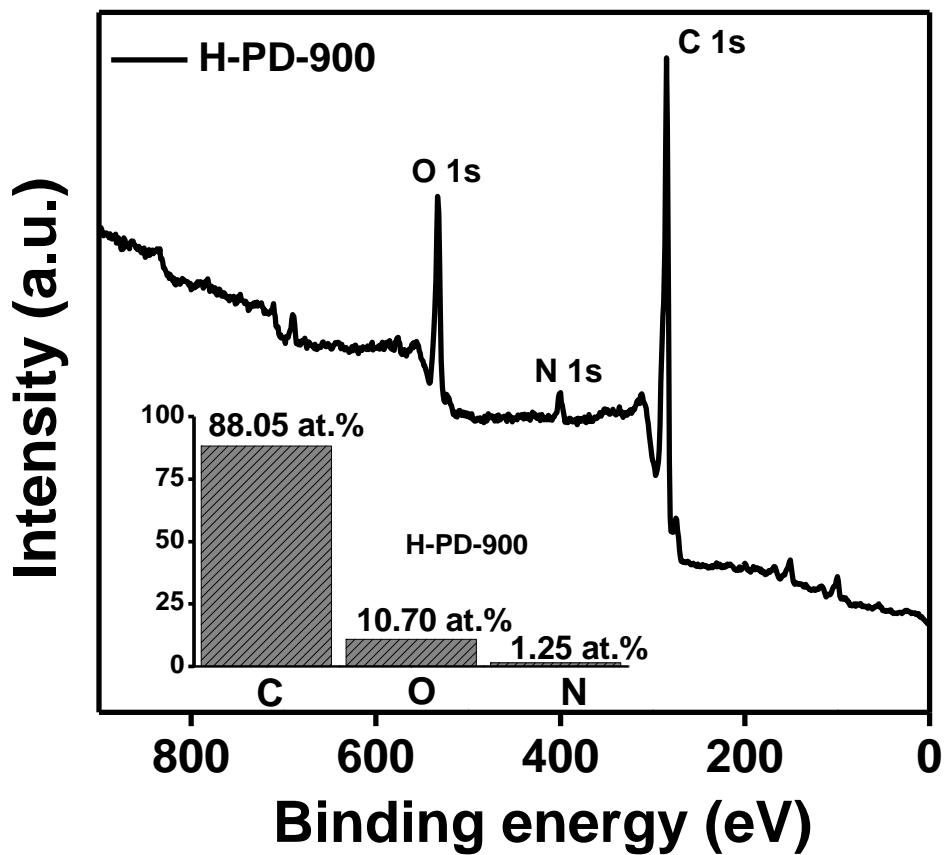


Figure S14. Deconvolution of high resolution N 1s XPS spectrum of NDC-700 indicating the presence of different N binding states.

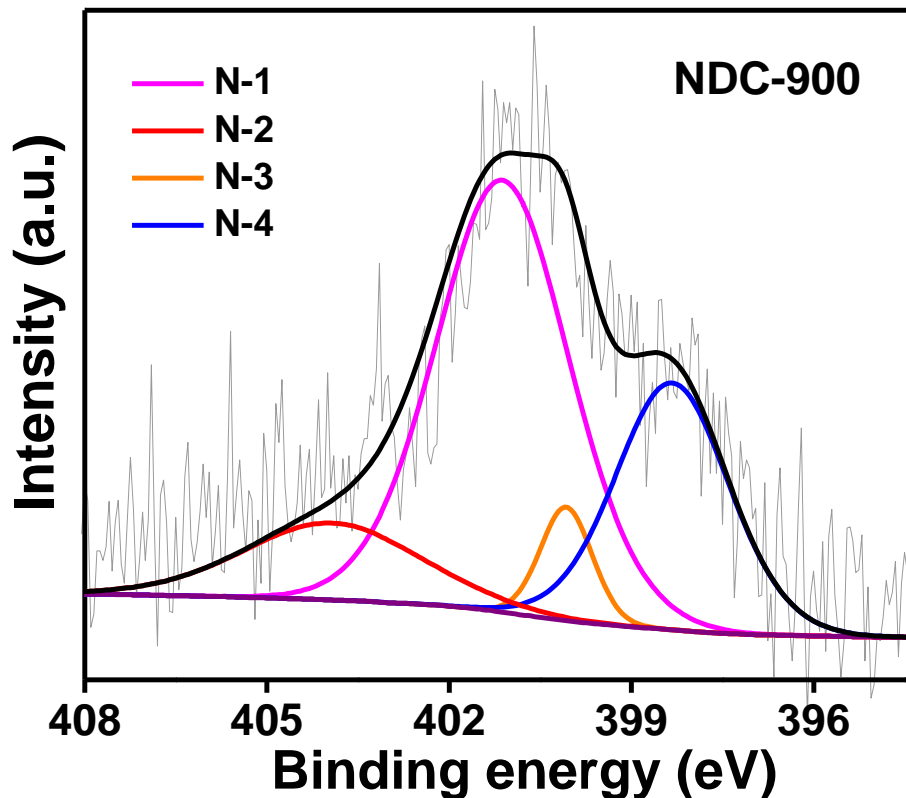


Figure S15. Deconvolution of high resolution N 1s XPS spectrum of NDC-900.

| Electocatalysts | N content (at. %) | Pyridinic-N (%) | Pyrrolic-N (%) | Graphitic-N (%) | Pyridinic N-oxide (%) |
|-----------------|----------------------|--------------------|-------------------|--------------------|--------------------------|
| NDC-700 | 5.20 | 33.27 | 16.43 | 42.41 | 7.89 |
| NDC-800 | 2.12 | 29.04 | 9.75 | 51.48 | 9.72 |
| NDC-900 | 1.25 | 26.66 | 5.57 | 54.81 | 12.96 |

Table S2. Percentage N content and relative percentages of different types of nitrogen in NDCs calculated from deconvolution of high resolution N 1s XPS spectra.

| Catalysts | η @ 10 mA cm ⁻² (mV vs. RHE) | Tafel Slope (mV dec ⁻¹) | Onset potential (mV vs. RHE) | j_o (mA cm ⁻²) | Ref. |
|---|---|--|---------------------------------|---|---------------------|
| NDC-800 | 276 | 94 | 117 | 1.50×10^{-2} | Present Work |
| N doped graphene | 490 | 116 | 330 | 7.01×10^{-5} | [1] |
| P doped graphene | 553 | 133 | 370 | 9.00×10^{-6} | [1] |
| N,P co-doped graphene | 420 | 91 | 289 | 2.44×10^{-4} | [1] |
| C,N architectures | 490 | 120 | ~200 | 1.45×10^{-2} | [2] |
| S doped graphene | 391 | 130 | 240 | 9.90×10^{-3} | [3] |
| N,S co-doped graphene | 276 | 81 | 130 | 8.40×10^{-3} | [3] |
| Core-shell MoO ₃ -MoS ₂ nanowires | 250 | 55 | 150-200 | 0.08×10^{-3} | [4] |
| Mesoporous double gyroid MoS ₂ | 250-300 | 50 | 150-200 | 0.69×10^{-3} | [5] |

Table S3. Comparison of HER parameters of some of the heteroatom doped carbon materials and non-precious transition metal chalcogenides with NDC-800.

Faradaic efficiency measurements:

Faradaic efficiency for the hydrogen evolution reaction was monitored by quantifying the amount of gas evolved as a function of time. Chronoamperometric measurements were performed -0.369 V vs. RHE using a typical H-shaped electrochemical cell in order to eliminate any contribution from oxygen reduction. Working electrode (modified by catalyst coating, NDC-800) and reference electrode (SCE) were kept in one compartment of H-cell while a large area Pt counter electrode was placed in the other (Figure S18). The quantity of gas evolved was measured using inverse burette method. It was observed that NDC-800 can produce around 7 mL of H₂ gas within 1.5 h. The amount of gas evolved during the reaction is in close agreement with the theoretical value, suggesting nearly 100% faradaic efficiency. Theoretically, the amount of H₂ gas evolved can be calculated from the equation based on Faraday's law (Equation 3) where I is the applied current, t is the time and F is Faraday constant, 96485.34 C.

$$\text{Moles of H}_2 = \frac{1}{2F} \int_0^t Idt \quad (3)$$

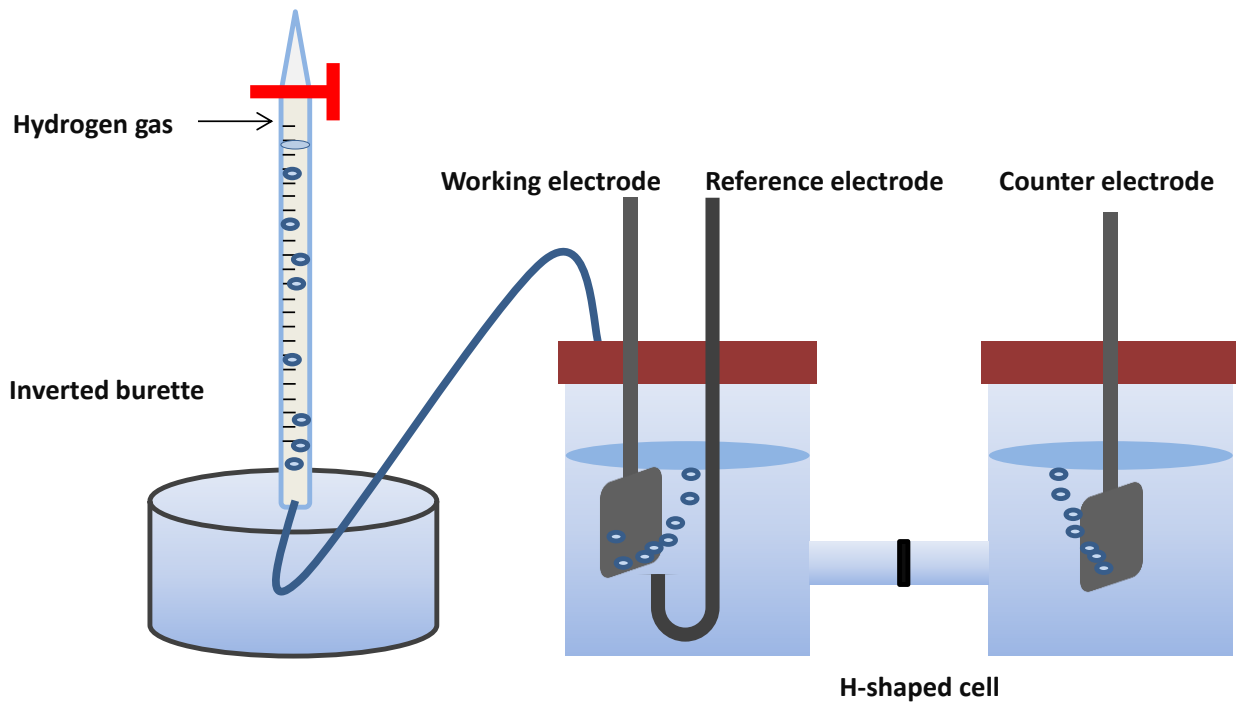


Figure S16. Schematic illustration of the experimental setup used for determining faradaic efficiency.

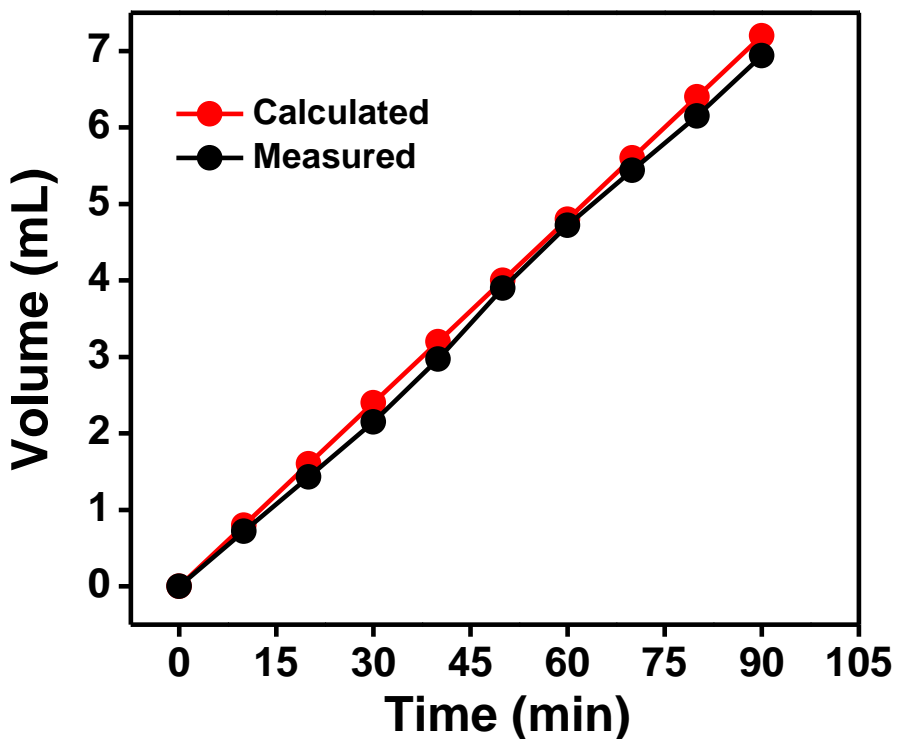


Figure S17. Amount of H_2 evolved as a function of time along with the expected values.

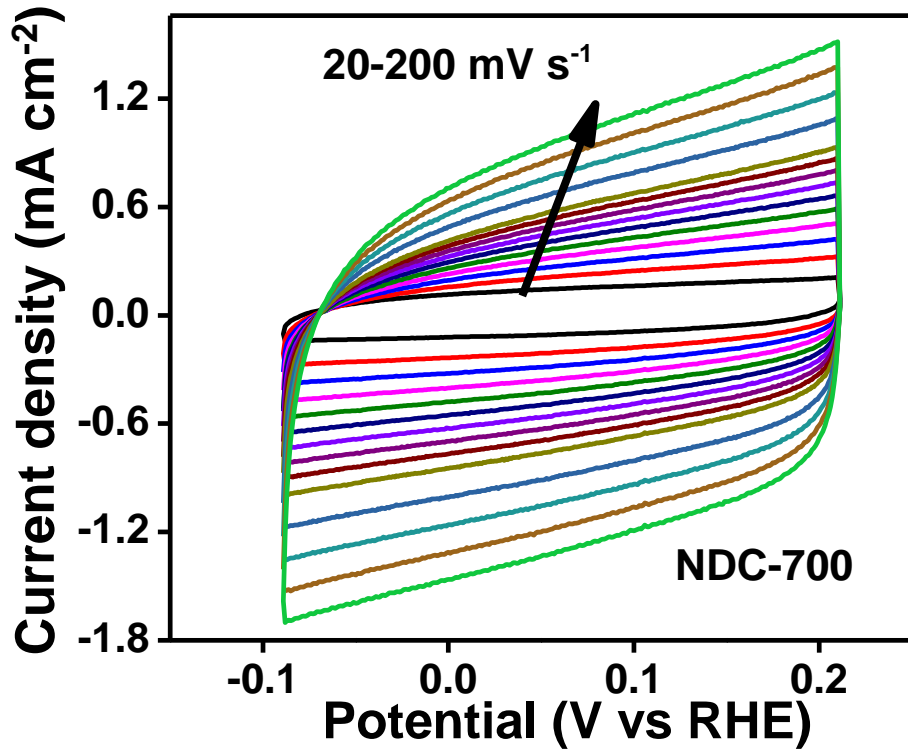


Figure S18. Cyclic voltammograms of NDC-700 at different scan rates.

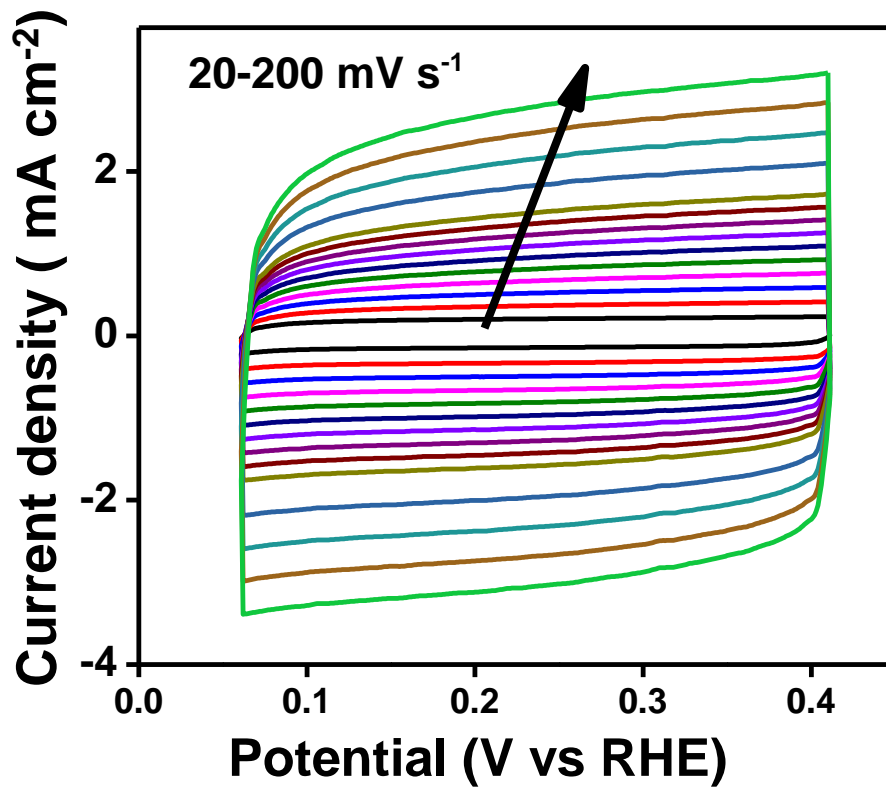


Figure S19. Cyclic voltammograms of NDC-900 at different scan rates.

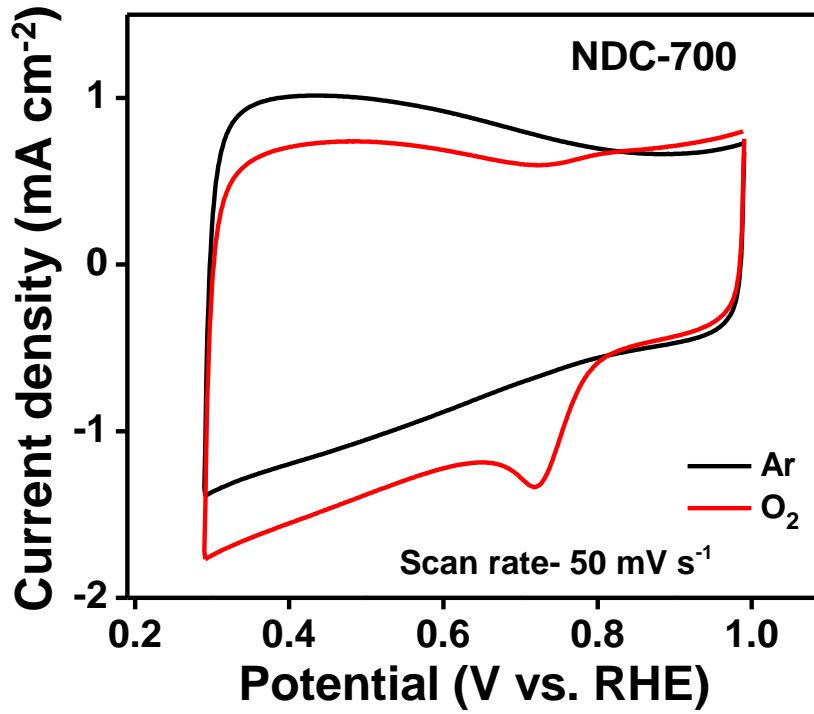


Figure S20. Cyclic voltammograms (CV) of NDC-700 in O_2 -saturated and Ar-saturated 0.1 M KOH at 50 mV s^{-1} .

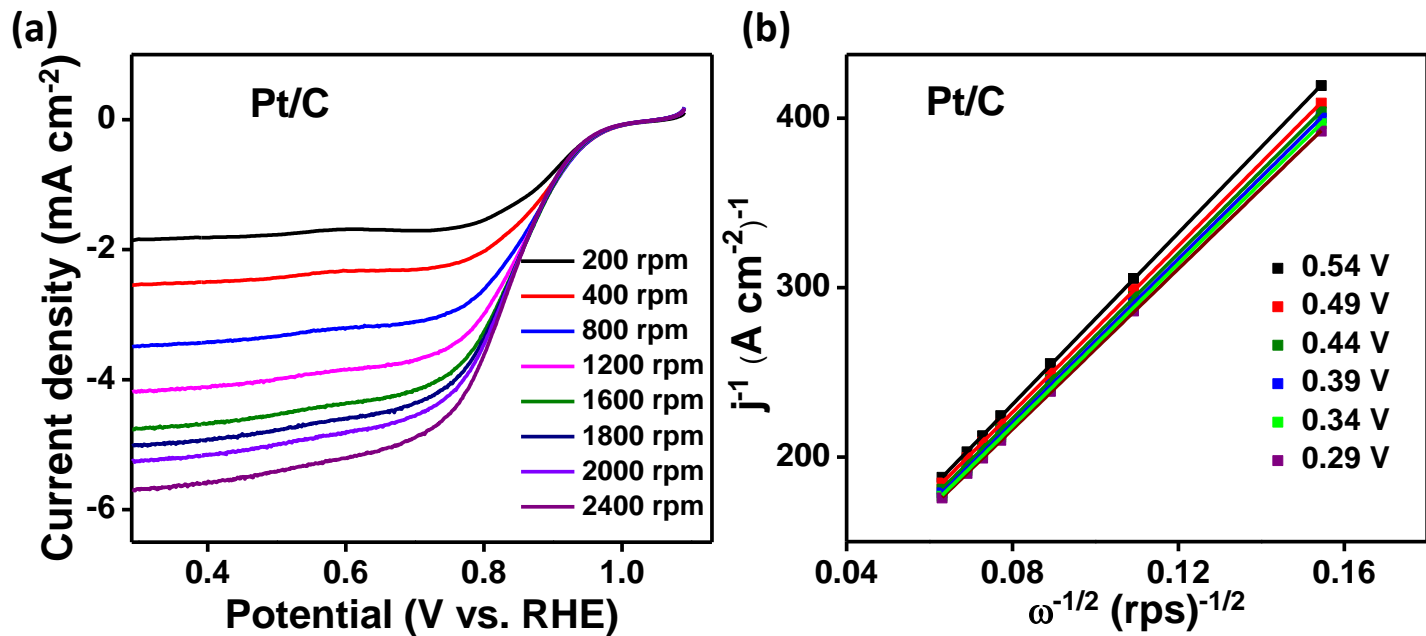


Figure S21. (a) Rotating disk electrode (RDE) voltammograms of Pt/C at different rotation rates in O_2 saturated 0.1 M KOH at 5 mV s^{-1} . (b) Shows corresponding Koutecky-Levich plots extracted from polarized LSV curves in (a).

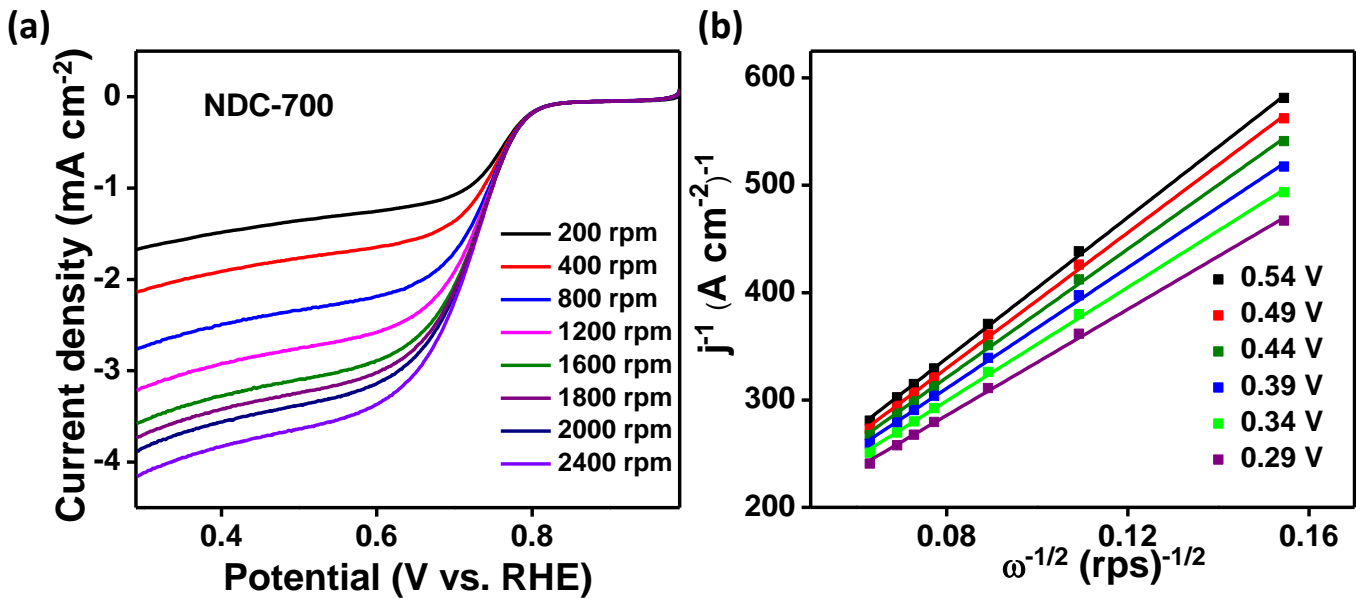


Figure S22. (a) Rotating disk electrode (RDE) voltammograms of NDC-700 at different rotation rates in O_2 saturated 0.1 M KOH at 5 mV s^{-1} . (b) Shows corresponding Koutecky-Levich plots extracted from polarized LSV curves in (a).

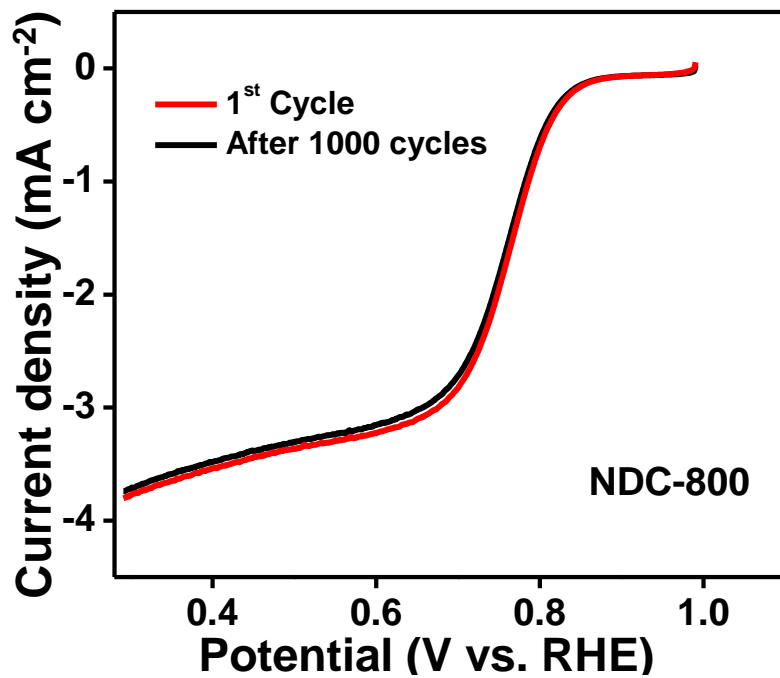


Figure S23. Comparison of linear sweep voltammograms (LSV) of NDC-800 at 1st cycle and after 1000 cycles.

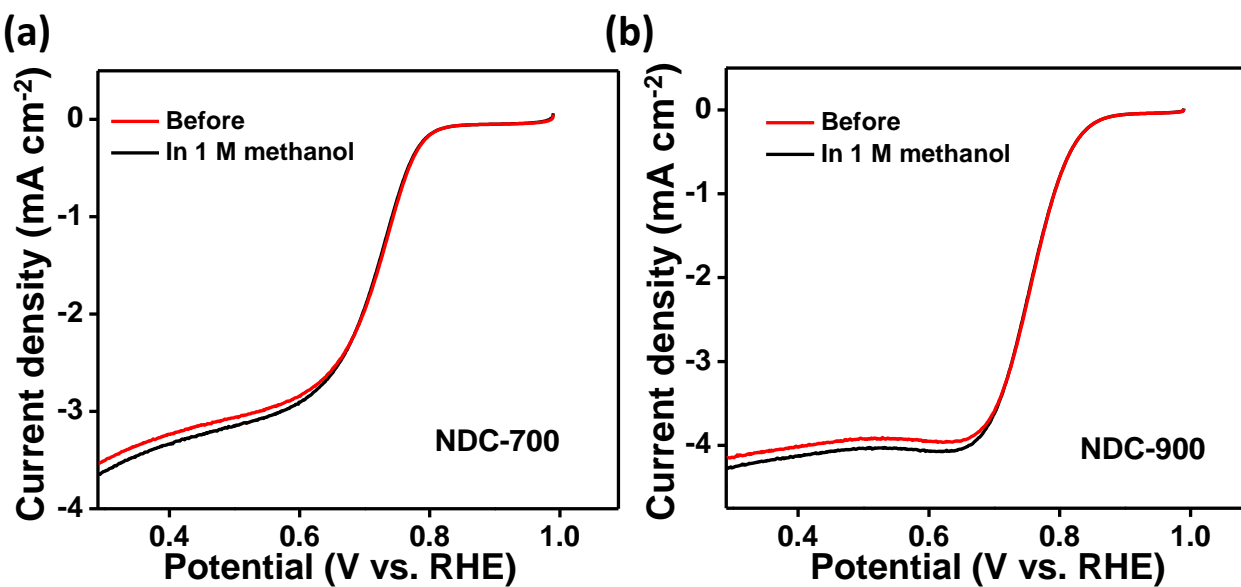


Figure S24. Linear sweep voltammograms (LSV) of NDC-700 (a) and NDC-900 (b), before and after addition of methanol to O_2 saturated 0.1 M KOH at 1600 rpm (5 mV s^{-1}).

References:

1. Y. Zheng, Y. Jiao, M. Jaroniec and S. Z. Qiao, *Angew. Chem. Int. Ed.*, 2015, **54**, 52-65.
2. K. Sakaushi and K. Uosaki, *ChemNanoMat*, 2016, **2**, 99-103.
3. Y. Ito, W. Cong, T. Fujita, Z. Tang and M. Chen, *Angew. Chem. Int. Ed.*, 2015, **54**, 2131-2136.
4. Z. Chen, D. Cummins, B. N. Reinecke, E. Clark, M. K. Sunkara and T. F. Jaramillo, *Nano Lett.*, 2011, **11**, 4168-4175.
5. J. Kibsgaard, Z. Chen, B. N. Reinecke and T. F. Jaramillo, *Nat Mater*, 2012, **11**, 963-969.